Published in final edited form as:
J Cardiovasc Electrophysiol. 2010 September ; 21(9): 1031–1037. doi:10.1111/j.1540-8167.2010.01736.x.

Diminished Cardiac Fibrosis in Heart Failure is Associated with Altered Ventricular Arrhythmia Phenotype

Jorge Massare, M.D.[*,§], **Jeff M. Berry, M.D.**[*,§], **Xiang Luo, M.D., Ph.D.**[*], **Farhana Rob, B.A.**[*], **Janet L. Johnstone, B.A.**[*], **John M. Shelton, B.Sc**[*], **Rhonda Bassel-Duby, Ph.D.**[†], **Joseph A. Hill, M.D., Ph.D.**[*,†], and **R. Haris Naseem, M.D.**[*,‡]

[*]Department of Internal Medicine (Cardiology), University of Texas Southwestern Medical Center, Dallas, Texas, USA

[†]Department of Molecular Biology, University of Texas Southwestern Medical Center, Dallas, Texas, USA

[‡]Department of Medicine, VA North Texas Health Care System, Dallas, Texas, USA

Abstract

Objectives—We sought to define the role of interstitial fibrosis in the proarrhythmic phenotype of failing ventricular myocardium.

Background—Multiple cellular events that occur during pathological remodeling of the failing ventricle are implicated in the genesis of ventricular tachycardia (VT), including interstitial fibrosis. Recent studies suggest that ventricular fibrosis is reversible, and current anti-remodeling therapies attenuate ventricular fibrosis. However, the role of interstitial fibrosis in the proarrhythmic phenotype of failing ventricular myocardium is currently not well defined.

Methods—Class II histone deacetylases (HDACs) have been implicated in promoting collagen biosynthesis. As these enzymes are inhibited by protein kinase D1 (PKD1), we studied mice with cardiomyocyte-specific transgenic over-expression of a constitutively activemutant of PKD1 (caPKD). caPKD mice were compared with animals in which cardiomyopathy was induced by severe thoracic aortic banding (sTAB). Hearts were analyzed by echocardiographic and electrocardiographic means. Interstitial fibrosis was assessed by histology and quantified biochemically. Ventricular arrhythmias were induced by closed-chest, intracardiac pacing.

Results—Similar degrees of hypertrophic growth, systolic dysfunction and mortality were observed in the two models. In sTAB mice, robust ventricular fibrosis was readily detected, but myocardial collagen content was significantly reduced in caPKD mice. As expected, VT was readily inducible by programmed stimulation in sTAB mice and VT was less inducible in caPKD mice. Surprisingly, episodes of VT manifested longer cycle lengths and longer duration in caPKD mice.

Address for correspondence: R. Haris Naseem, M.D., Division of Cardiology, UT Southwestern Medical Center, NB11.200, 6000 Harry Hines Blvd., Dallas, TX 75390-8573. Fax: 214-648-1450; Rao.naseem@UTsouthwestern.edu.
[§]Authors contributed equally to this work.

No disclosures.

Supporting Information

Additional Supporting Information may be found in the online version of this article:

Tabel S1. Electrophysiological parameters in WT, sTAB, and caPKD mice.

Please note: Wiley-Blackwell is not responsible for the content or functionality of any supporting materials supplied by the authors. Any queries (other than missing material) should be directed to the corresponding author for the article.

Conclusion—Attenuated ventricular fibrosis is associated with reduced VT inducibility, increased VT duration, and significantly longer arrhythmia cycle length.

Keywords

dilated cardiomyopathy; fibrosis; ventricular tachycardia; histone deacetylases; protein kinase D

Introduction

The mammalian heart undergoes profound remodeling when subjected to abnormal stress, such as that associated with hypertension or myocardial infarction.[1] This remodeling process includes cardiomyocyte hypertrophy, transformation of fibroblasts to myofibroblasts, extracellular matrix (ECM) deposition, interstitial fibrosis, alteration in cardiac gene expression, and cell death.[2–4] These remodeling processes are associated with adverse events, including a markedly increased risk of heart failure, ventricular arrhythmias and sudden cardiac death.[5] Excessive cardiac fibrosis contributes to cardiac dysfunction and, in addition, plays an important role in ventricular arrhythmogenesis.[6,7]

Genomic DNA within eukaryotic cells is highly compacted with histone and nonhistone proteins in a dynamic polymer called chromatin. Acetylation of lysine residues in histone tails by histone acetyltransferases (HATs) stimulates gene expression by facilitating access of transcription factors to DNA. The stimulatory effect of HATs on gene expression is countered by histone deacetylases (HDACs), which promote chromatin condensation and thereby repress transcription.[8] HDAC inhibition blunts pressure overload-induced cardiac hypertrophy with significant reduction in myocardial fibrosis.[9] Protein kinase D1 (PKD1) is an HDAC kinase that participates in pathological cardiac remodeling, and inhibits HDAC activity by promoting the export of class II HDACs from the nucleus to the cytoplasm.[10,11] Over-expression of PKD1 in the mouse heart leads to heart failure with minimal cardiac fibrosis.[12] The electrophysiological phenotype of pathological cardiac remodeling with diminished cardiac fibrosis is currently unknown.

Two independently regulated biological factors contribute to cardiac structural remodeling and arrhythmogenesis—changes in membrane protein composition and fibrosis. Myocardial fibrosis, in turn, promotes ventricular arrhythmogenesis through multiple mechanisms.[13–16] Recent work suggests that cardiac fibrosis, long held to be irreversible, may regress under certain conditions.[17] Also, several current therapies for heart failure elicit declines in both fibrosis and sudden cardiac death.[4] With the emergence of therapeutic strategies that target fibrosis, including therapies presently in clinical use (aldosterone antagonists,[18–20] ACE inhibitors,[21] statins[21]) and those in preclinical development (HDAC inhibitors[9]), we set out to parse the role of interstitial fibrosis in the proarrhythmic phenotype of the failing myocardium. To accomplish this, we employed a novel model of heart failure that is generated by cardiomyocyte-specific over-expression of a constitutively active mutant of PKD1 (caPKD).[12]

Materials and Methods

Animal Care

Adult male C57BL/6 and PKD (B6 background) transgenic mice 8–10 weeks of age were used in these studies. Mice were bred and housed in cages, and all animal protocols were in accordance with our institutional animal care guidelines. The institutional animal care committee approved all animal protocols.

Severe Thoracic Aortic Banding

Increased pressure in the proximal aorta was induced by means of severe thoracic aortic banding (sTAB).[22] Briefly, male C57BL6 (6–8 weeks old) were anesthetized with ketamine (100 mg/kg IP) plus xylazine (5 mg/kg IP). The mice were then orally intubated with 20-gauge tubing and ventilated (Harvard Apparatus Rodent Ventilator, model 687) at 120 breaths per minute (0.1 mL tidal volume). A 3-mm left sided thoracotomy was created at the second intercostal space. The transverse aortic arch was ligated (7–0 Prolene) between the innominate and left common carotid arteries with an overlying 28-gauge needle, and then the needle was removed, leaving a discrete region of stenosis. The chest was closed, and the left sided pneumothorax was evacuated. Perioperative (24 hours) mortality was <10%.

Histology

Adult mice were anesthetized with Avertin and perfusion fixed transcardially with 4% paraformaldehyde-PBS. The hearts were harvested and postfixed for 90 minutes at room temperature, rinsed in diethyl pyrocarbonate-PBS, and paraffin processed. Paraffin sections (5 μm) were mounted on silanated glass and selected sections were stained by hematoxylin-eosin or Masson's trichrome stain according to established protocols.[23]

Hydroxyproline Assay

Hydroxyproline analysis was carried out based on the method described.[24] Briefly, hearts were harvested from wild type and PKD transgenic animals, the left ventricle was dissected free, and tissue was lyophilized. Equal amounts of this lyophilized tissue (approximately 25 mg per sample) were suspended in 6 N HCl, and hydrolyzed at 120°C. Samples were neutralized with 4 N NaOH. Samples and standards (L-hydroxyproline, Sigma) were incubated for 20 minutes at room temperature with chloramine T, followed by addition of Ehrlich reagent (3.75 g of p-dimethylaminobenzaldehyde, 15 ml of 1-propanol, 6.5 ml of perchloric acid (60%) in 25 mL for 20 min at 60°C. Absorbances were read at $\lambda = 558$ nm. Values were calculated from a standard curve generated for each analysis. Results are expressed as microgram of hydroxyproline per milligram of dried tissue sample.

Echocardiography

Transthoracic echocardiograms were recorded in conscious mice as described.[25,26] In brief, views were taken in planes which approximated the parasternal short-axis view (chordal level) and the apical long-axis view in humans. LV internal diameters and wall thicknesses were measured (at least 3 cardiac cycles) at end-systole and end-diastole. Fractional shortening was calculated from M-mode images as the left ventricular end-diastolic dimension (LVEDD) minus the left ventricular end-systolic dimension (LVESD) divided by LVEDD.

Cellular Electrophysiological Recordings

Mice LV cardiomyocytes were isolated using enzymatic digestion and mechanical dispersion methods previously described.[27] In brief, after retrograde perfusion with Ca^{2+}-free buffer and following collagenase solution, the LV tissue was separated using a fine scalpel and scissors. After gentle trituration, cells were plated and studied within 6 hours at room temperature. Whole cell current clamp experiments (Axopatch 200B, Molecular Devices) were conducted to measure cardiomyocytes membrane action potentials (AP). Cells were plated in a chamber that was superfused at 1 to 2 mL/min with standard solution A containing 140 mM NaCl, 5 mMKCl, 1 mM $MgCl_2$, 1 mM $CaCl_2$, 10 mMHEPES (pH 7.4 with NaOH), and 10 mM glucose (310 mOsm). Only calcium-tolerant, quiescent, and rod-shaped cells showing clear cross-striations were studied. Recording pipettes were prepared with resistances of 2–3 MΩ when filled with internal solution containing 135 mM KCl, 10

mM EGTA, 10 mM HEPES, 5 mM glucose (pH7.2 with KOH; 300 mOsm). Action potentials were recorded in response to brief (1~2 ms) depolarizing current (1~2 nA) injections delivered at 1 Hz. All data were filtered at 5kHz and analyzed by pCLAMP 9 software (Molecular Devices).

Electrophysiological Studies

Mice were sedated by intraperitoneal administration of pentobarbital (0.050 mg/g). Transvenous electrophysiological studies were performed according to procedures previously described.[28] Following tracheal intubation, mice were mechanically ventilated using a mouse ventilator (Harvard Apparatus Model 687). The right jugular vein was exposed, and a 1.1 F octapolar EP catheter (Millar EPR-800) was inserted transvenously into the right jugular vein and advanced to the right atrium or right ventricle using electrogram tracings for guidance. The EP catheter included 8 electrodes with 1.0 mm electrode spacing, and the distal electrode pair was used to stimulate while recording from all other electrodes.

A standard 6-lead surface ECG was recorded during pacing using needle electrodes attached to each limb of the mouse. Standard pacing protocols, including programmed electrical stimulation, were used to determine electrophysiological parameters. Ventricular extra-stimulation was performed to measure ventricular refractory periods and attempt to induce ventricular arrhythmias. Single extrastimuli were introduced after a drive train of 8 beats, and the S1-S2 interval was decremented in 5 msec steps until refractory. With the S1–S2 interval 10 msec above refractoriness, double extrastimuli were then introduced, decrementing the S2–S3 interval by 5 msec until refractory. Next triple extrastimuli were introduced in a similar fashion decrementing the S3–S4 interval by 5 msec until refractory. Each stimulus train was repeated twice, and the EP study was continued until either VT was induced or all stimuli were completed. VT in this study is defined as at least 4 wide QRS beats after the last paced beat occurring at a rate faster than 600 bpm. If VT was induced, the stimuli were repeated twice to demonstrate reproducibility. This same pacing protocol was performed in all animals. The operator remained blinded to genotype during the performance of and interpretation of studies.

Statistical Analysis

Wild type B6 and transgenic caPKD mice were compared to gender- and age-matched control mice. Standard cardiac conduction times were compared, with data presented as the mean ± standard deviation. Statistical analyses included use of the 2-tailed Student’s t-test for continuous variables and Fisher exact test for categorical variables. Differences in mean values were reported as significant if the P value was <0.05.

Results

caPKD and sTAB Models of Cardiomyopthy Have Similar Levels of Cardiac Dysfunction

We first evaluated the models for the extent of cardiomyopathy that develops in sTAB hearts 3 weeks after surgery as compared with 8 weeks of transgene activation in the case of caPKD over-expressing mice. caPKD and sTAB mice manifested similar degrees of cardiac dilation and dysfunction with comparable decreases in left ventricular fractional shortening and increased systolic dimensions (Fig. 1A–C). In addition, both of these models exhibited increases in heart weight to body weight ratio, which were comparable and significantly greater than their wild type, unoperated counterparts (Fig. 1D). Resting baseline EKGs under sedated conditions were also compared between the two models. Apart from a modest increase in PR interval in caPKD hearts, no significant differences were seen between the 2 models of cardiomyopathy (Fig. 1E).

caPKD and sTAB Models of Cardiomyopthy Have Similar Cellular Electrophysiological Properties

Since sTAB and caPKD mice have similar levels of dilated cardiomyopathy, we pursued cellular electrophysiological evaluation of the 2 models. Apart from a modest increase in ventricular effective refractory period in caPKD heart (47.92 ± 11.4 msec in caPKD and 35.83 ± 7.36 msec, $P < 0.05$) other electrocardiographic and in vivo electrophysiological parameters were equivalent in the 2 models of heart failure (Supporting Table S1).

To further investigate the electrophysiological substrate in caPKD and sTAB animals, we recorded myocyte action potentials. Consistent with surface electrocardiographic findings, the action potential duration was prolonged in both caPKD and sTAB mice as compared with wild type mice (Fig. 2A). Action potential duration at 30% repolarization (APD 30) and action potential duration at 90% repolarization (APD 90) were similar in the two models of dilated cardiomyopathy, and significantly increased as compared with wild type mice (Fig. 2B).

Diminished Myocardial Fibrosis in caPKD Over-Expression Induced Cardiomyopathy

After establishing that the 2 experimental models manifested similar degrees of dilated cardiomyopathy with comparable electrocardiographic and cellular electrophysiological changes, we assessed the left ventricles for fibrosis. Initial descriptions of caPKD over-expressing mice suggested diminished fibrosis.[12] To pursue this further, we performed a comprehensive analysis of the amount of fibrosis in each model. Histological analysis of sTAB and caPKD hearts, using trichrome staining, showed that while sTAB animals manifested significant fibrosis, minimal fibrosis was seen in caPKD hearts (Fig. 3A). Wild type and sham-operated animals did not manifest significant myocardial fibrosis under baseline conditions. Hearts from WT, caPKD and sTAB animals were then assessed biochemically for collagen content using a hydroxyproline assay. This quantitative assay confirmed our histological findings and showed that caPKD hearts have significantly less fibrosis despite similar degrees of heart failure (Fig. 3B).

PKD Over-Expressing Mice Have Less Inducible Ventricular Arrhythmias

To assess in vivo effects of altered fibrosis in the setting of dilated cardiomyopathy, we performed EP studies with and without isoproterenol infusion. Consistent with a prior report,[29] we were not able to induce ventricular arrhythmias in wild type C57BL/6 mice despite aggressive pacing protocols with or without isoproterenol. In contrast, ventricular arrhythmias were readily induced by programmed stimulation in both sTAB and caPKD mice (Fig. 4A). Quantitative evaluation revealed that ventricular tachycardia was significantly less readily induced in caPKD mice as compared with sTAB animals (Fig. 4B).

Electrophysiological Characteristics of Induced Ventricular Arrhythmias Differ Between caPKD Mice and sTAB Mice

Next, we analyzed the characteristics and duration of inducible arrhythmias in the 2 animal models. The average duration of induced ventricular tachycardias was markedly longer in caPKD mice compared with the sTAB model of dilated cardiomyopathy (mean duration of induced VT in caPKD mice was 1833 ± 723 msec vs. 373 ± 200 msec in sTAB mice, $P < 0.05$) (Fig. 5A and Supporting Table S1). In addition the cycle length of VT was significantly longer in caPKD mice compared with sTAB animals (mean cycle length of VT in caPKD mice was 58 ± 4 msec vs. 49 ± 1 msec in sTAB mice, $P < 0.05$) (Fig. 5B and Supporting Table S1).

Discussion

Cardiac fibrosis is a hallmark of structural remodeling in response to a variety of stressors and central to arrhythmogenesis in the pathologically remodeled heart. The major findings we describe here are (a) caPKD over-expression leads to dilated cardiomyopathy with diminished fibrosis despite similar levels of cardiomyopathy as induced by pressure overload; (b) ventricular tachycardia inducibility is significantly decreased in a model of dilated cardiomyopathy with limited myocardial scar; (c) ventricular arrhythmias have prolonged duration and decreased rate in cardiomyopathy with reduced fibrosis. Together, these results suggest a previously unknown electrophysiological phenotype of dilated cardiomyopathy in the setting of diminished fibrosis.

Fibrosis is a hallmark feature of the pathologically remodeled ventricle, contributing to both diastolic and systolic contractile dysfunction and arrhythmogenesis.[4,13] A variety of sources contribute to the fibroblast population within the heart in response to stress, including resident cardiac fibroblasts, cells of bone marrow origin, and fibroblasts that originate from cardiac endothelial cells (endothelia-mesenchymal transition).[17] In response to myocardial stress, these fibroblasts differentiate into myofibroblasts, and transforming growth factor-β1 (TGFβ), amolecule prominently activated by stress, facilitates this process along with stimulating collagen secretion.[30] The resulting collagenous septa and ventricular myofibroblasts both have been shown conclusively to facilitate the arrhythmic phenotype of the remodeled myocardium.[14–16] Therefore, it is not surprising that recent investigations have targeted the fibrotic scar of the heart to manipulate the structure and arrhythmic phenotype of the remodeled heart.[31–33]

It is well established that increased amounts of fibrotic tissue in the heart are strongly correlated with an increased incidence of atrial and ventricular tachyarrhythmias and sudden cardiac death.[21,34] Current therapies that reduce the amount of fibrosis, as a component of their mechanism have been shown already to diminish sudden cardiac death rates.[35] Our findings suggest that at least in part, a reduction in VT induction and alteration of VT phenotype could account for the observed reduction in sudden cardiac death rates. However, although our findings are highly suggestive they do not establish a cause and effect relationship and further work needs to be done prior to making that conclusion clearly. While the 2 models we have used in this study, caPKD and sTAB, differ significantly in the amount of fibrosis, other potential differences might contribute to these findings. One such difference is the effect of PKD1 on L type voltage gated calcium channel that has been recently described.[36] It is possible that this association might lead to functional changes that could account for some of the observed findings a lack of significant differences in cellular action potentials might argue against it.

In addition, we have demonstrated that arrhythmias in a fibrosis-deficient model of cardiomyopathy propagate for longer durations as compared to those in a pressure-overload model of cardiomyopathy. We have also shown that induced ventricular arrhythmias manifest longer cycle lengths (diminished rate) in these hearts. This is a surprising and potentially important finding as new antifibrotic therapies are developed, especially in light of growing evidence for the significant impact that fibrosis has on induction and propagation of conduction.[37] Indeed, our findings support a complex role that myocardial scar plays in ventricular arrhythmogenesis. Whereas our results suggest that fibrotic scar is arrhythmogenic, it conceivably may also play a “protective” role in limiting propagation of ventricular arrhythmias. In recent years, significant progress has been made in developing therapeutic strategies designed to abort tachyarrhythmias as they develop.[38] However, many questions remain before envisioning disease-based therapy that targets the proarrhythmic phenotype itself. Given the recently established role of fibrosis, cardiac fibrosis has emerged

as a potential target for anti arrhythmic therapies. In fact, several antifibrotic therapies are either in clinical use presently or in preclinical development.[35,39] Likely these therapies will lead to altered fibrosis levels in the failing heart and thereby modify the electrical properties of hypertrophied or failing hearts. As these antifibrotic therapies are emerging, their impact on the arrhythmic substrate of the myocardium is critical to understand. In summary, our findings indicate that use of antifibrotic therapies without a clear knowledge and understanding of their impact on fibrosis might convert one electrical abnormality to another.

Limitations

The 2 animal models of cardiomyopathy that we evaluated, caPKD and sTAB, are similar in structure, function, and cellular electrophysiological parameters but differ in the amount of myocardial fibrosis. However, we have not ruled out differences in individual channel expression and ion currents that might exist though similarities in cellular recordings would suggest that even if such differences exist, they do not contribute significantly to the overall action potential.

Supplementary Material

Refer to Web version on PubMed Central for supplementary material.

Acknowledgments

We thank Dr. Eric Olson (University of Texas Southwestern Medical Center, Dallas, Texas) for critical review of the manuscript.

This work was supported by the Heart Rhythm Society (Fellowship grant to JM); American Heart Association 0705170Y, 0830313N (RHN), 0640084N JAH); Donald W. Reynolds Foundation (J.A.H.) and National Institutes of Health Grants HL-075173, HL-006296, and HL-080144 (J.A.H.).

References

1. Hill JA, Olson EN. Cardiac plasticity. N Engl J Med. 2008; 358:1370–1380. [PubMed: 18367740]
2. Frey N, Olson EN. Cardiac hypertrophy: The good, the bad, and the ugly. Annu Rev Physiol. 2003; 65:45–79. [PubMed: 12524460]
3. Nass RD, Aiba T, Tomaselli GF, Akar FG. Mechanisms of disease: Ion channel remodeling in the failing ventricle. Nat Clin Pract Cardiovas Med. 2008; 5:196–207.
4. Spinale FG. Myocardial matrix remodeling and the matrix metal-loproteinases: Influence on cardiac form and function. Physiol Rev. 2007; 87:1285–1342. [PubMed: 17928585]
5. Tomaselli GF, Zipes DP. What causes sudden death in heart failure? Circ Res. 2004; 95:754–763. [PubMed: 15486322]
6. Manabe I, Shindo T, Nagai R. Gene expression in fibroblasts and fibrosis: Involvement in cardiac hypertrophy. Circ Res. 2002; 91:1103–1113. [PubMed: 12480810]
7. Weber KT. Fibrosis in hypertensive heart disease: Focus on cardiac fibroblasts. J Hypertens. 2004; 22:47–50. [PubMed: 15106793]
8. Backs J, Olson EN. Control of cardiac growth by histone acetylation/deacetylation. Circ Res. 2006; 98:15–24. [PubMed: 16397154]
9. Kong Y, Tannous P, Lu G, Berenji K, Rothermel BA, Olson EN, Hill JA. Suppression of class I and II histone deacetylases blunts pressure-overload cardiac hypertrophy. Circulation. 2006; 113:2579–2588. [PubMed: 16735673]
10. Vega RB, Harrison BC, Meadows E, Roberts CR, Papst PJ, Olson EN, McKinsey TA. Protein kinases C and D mediate agonist-dependent cardiac hypertrophy through nuclear export of histone deacetylase 5. Mol Cell Biol. 2004; 24:8374–8385. [PubMed: 15367659]

11. Fielitz J, Kim MS, Shelton JM, Qi X, Hill JA, Richardson JA, Bassel-Duby R, Olson EN. Requirement of protein kinase D1 for pathological cardiac remodeling. Proc Natl Acad Sci USA. 2008; 105:3059–3063. [PubMed: 18287012]
12. Harrison BC, Kim MS, van Rooij E, Plato CF, Papst PJ, Vega RB, McAnally JA, Richardson JA, Bassel-Duby R, Olson EN, McKinsey TA. Regulation of cardiac stress signaling by protein kinase d1. Mol Cell Biol. 2006; 26:3875–3888. [PubMed: 16648482]
13. Zeppenfeld K, Stevenson WG. Ablation of ventricular tachycardia in patients with structural heart disease. Pacing Clin Electrophysiol. 2008; 31:358–374. [PubMed: 18307634]
14. Spach MS, Boineau JP. Microfibrosis produces electrical load variations due to loss of side-to-side cell connections: A major mechanism of structural heart disease arrhythmias. Pacing Clin Electrophysiol. 1997; 20:397–413. [PubMed: 9058844]
15. Miragoli M, Gaudesius G, Rohr S. Electrotonic modulation of cardiac impulse conduction by myofibroblasts. Circ Res. 2006; 98:801–810. [PubMed: 16484613]
16. Miragoli M, Salvarani N, Rohr S. Myofibroblasts induce ectopic activity in cardiac tissue. Circ Res. 2007; 101:755–758. [PubMed: 17872460]
17. Zeisberg EM, Tarnavski O, Zeisberg M, Dorfman AL, McMullen JR, Gustafsson E, Chandraker A, Yuan X, Pu WT, Roberts AB, Neilson EG, Sayegh MH, Izumo S, Kalluri R. Endothelial-to-mesenchymal transition contributes to cardiac fibrosis. Nat Med. 2007; 13:952–961. [PubMed: 17660828]
18. Brilla CG, Matsubara LS, Weber KT. Anti-aldosterone treatment and the prevention of myocardial fibrosis in primary and secondary hyper-aldosteronism. J Mol Cell Cardiol. 1993; 25:563–575. [PubMed: 8377216]
19. Lea WB, Kwak ES, Luther JM, Fowler SM, Wang Z, Ma J, Fogo AB, Brown NJ. Aldosterone antagonism or synthase inhibition reduces end-organ damage induced by treatment with angiotensin and high salt. Kidney Int. 2009:1523–1755. Epub Feb.
20. Van Den Borne SW, Isobe S, Zandbergen HR, Li P, Petrov A, Wong ND, Fujimoto S, Fujimoto A, Lovhaug D, Smits JF, Daemen MJ, Blankesteijn WM, Reutelinsgsperger C, Zannad F, Narula N, Vannan MA, Pitt B, Hofstra L, Narula J. Molecular imaging for efficacy of pharmacologic intervention in myocardial remodeling. JACC Cardiovasc Imaging. 2009; 2:187–198. [PubMed: 19356555]
21. Everett, THt; Olgin, JE. Atrial fibrosis and the mechanisms of atrial fibrillation. Heart Rhythm. 2007; 4(3 Suppl):S24–S27. [PubMed: 17336879]
22. Rothermel BA, Berenji K, Tannous P, Kutschke W, Dey A, Nolan B, Yoo KD, Demetroulis E, Gimbel M, Cabuay B, Karimi M, Hill JA. Differential activation of stress-response signaling in load-induced cardiac hypertrophy and failure. Physiol Genomics. 2005; 23:18–27. [PubMed: 16033866]
23. Woods, AE.; Ellis, RC. Laboratory Histopathology, A Complete Reference. Churchill: Livingston Press; 1996.
24. Woessner JF Jr. The determination of hydroxyproline in tissue and protein samples containing small proportions of this imino acid. Arch Biochem Biophys. 1961; 93:440–447. [PubMed: 13786180]
25. Hill JA, Karimi M, Kutschke W, Davisson RL, Zimmerman K, Wang Z, Kerber RE, Weiss RM. Cardiac hypertrophy is not a required compensatory response to short-term pressure overload. Circulation. 2000; 101:2863–2869. [PubMed: 10859294]
26. Hill JA, Rothermel B, Yoo KD, Cabuay B, Demetroulis E, Weiss RM, Kutschke W, Bassel-Duby R, Williams RS. Targeted inhibition of calcineurin in pressure-overload cardiac hypertrophy. Preservation of systolic function. J Biol Chem. 2002; 277:10251–10255. [PubMed: 11786544]
27. Wang Y, Tandan S, Cheng J, Yang C, Nguyen L, Sugianto J, Johnstone JL, Sun Y, Hill JA. Ca2+/calmodulin-dependent protein kinase II-dependent remodeling of Ca2+ current in pressure overload heart failure. J Biol Chem. 2008; 283:25524–25532. [PubMed: 18622016]
28. Berul CI, Christe ME, Aronovitz MJ, Maguire CT, Seidman CE, Seidman JG, Mendelsohn ME. Familial hypertrophic cardiomyopathy mice display gender differences in electrophysiological abnormalities. J Interv Card Electrophysiol. 1998; 2:7–14. [PubMed: 9869991]

29. Maguire CT, Wakimoto H, Patel VV, Hammer PE, Gauvreau K, Berul CI. Implications of ventricular arrhythmia vulnerability during murine electrophysiology studies. Physiol Genomics. 2003; 15:84–91. [PubMed: 12888626]
30. Petrov VV, Fagard RH, Lijnen PJ. Stimulation of collagen production by transforming growth factor-beta1 during differentiation of cardiac fibroblasts to myofibroblasts. Hypertension. 2002; 39:258–263. [PubMed: 11847194]
31. Laflamme MA, Murry CE. Regenerating the heart. Nat Biotechnol. 2005; 23:845–856. [PubMed: 16003373]
32. Duffy HS. Cardiac connections–the antiarrhythmic solution? N Engl J Med. 2008; 358:1397–1398. [PubMed: 18367745]
33. Roell W, Lewalter T, Sasse P, Tallini YN, Choi BR, Breitbach M, Doran R, Becher UM, Hwang SM, Bostani T, von Maltzahn J, Hofmann A, Reining S, Eiberger B, Gabris B, Pfeifer A, Welz A, Willecke K, Salama G, Schrickel JW, Kotlikoff MI, Fleischmann BK. Engraftment of connexin 43-expressing cells prevents post-infarct arrhythmia. Nature. 2007; 450:819–824. [PubMed: 18064002]
34. Varnava AM, Elliott PM, Mahon N, Davies MJ, McKenna WJ. Relation between myocyte disarray and outcome in hypertrophic cardiomyopathy. Am J Cardiol. 2001; 88:275–279. [PubMed: 11472707]
35. Brown RD, Ambler SK, Mitchell MD, Long CS. The cardiac fibroblast: Therapeutic target in myocardial remodeling and failure. Ann Rev Pharmacol Toxicol. 2005; 45:657–687. [PubMed: 15822192]
36. Maturana AD, Walchli S, Iwata M, Ryser S, Van Lint J, Hoshijima M, Schlegel W, Ikeda Y, Tanizawa K, Kuroda S. Enigma homolog 1 scaffolds protein kinase D1 to regulate the activity of the cardiac L-type voltage-gated calcium channel. Cardiovasc Res. 2008; 78:458–465. [PubMed: 18296710]
37. Ten Tusscher KH, Panfilov AV. Influence of diffuse fibrosis on wave propagation in human ventricular tissue. Europace. 2007; 9(Suppl 6):vi38–vi45. [PubMed: 17959692]
38. Darbar D, Roden DM. Future of antiarrhythmic drugs. Curr Opin Cardiol. 2006; 21:361–367. [PubMed: 16755206]
39. Berry JM, Cao DJ, Rothermel BA, Hill JA. Histone deacetylase inhibition in the treatment of heart disease. Expert Opin Drug Saf. 2008; 7:53–67. [PubMed: 18171314]

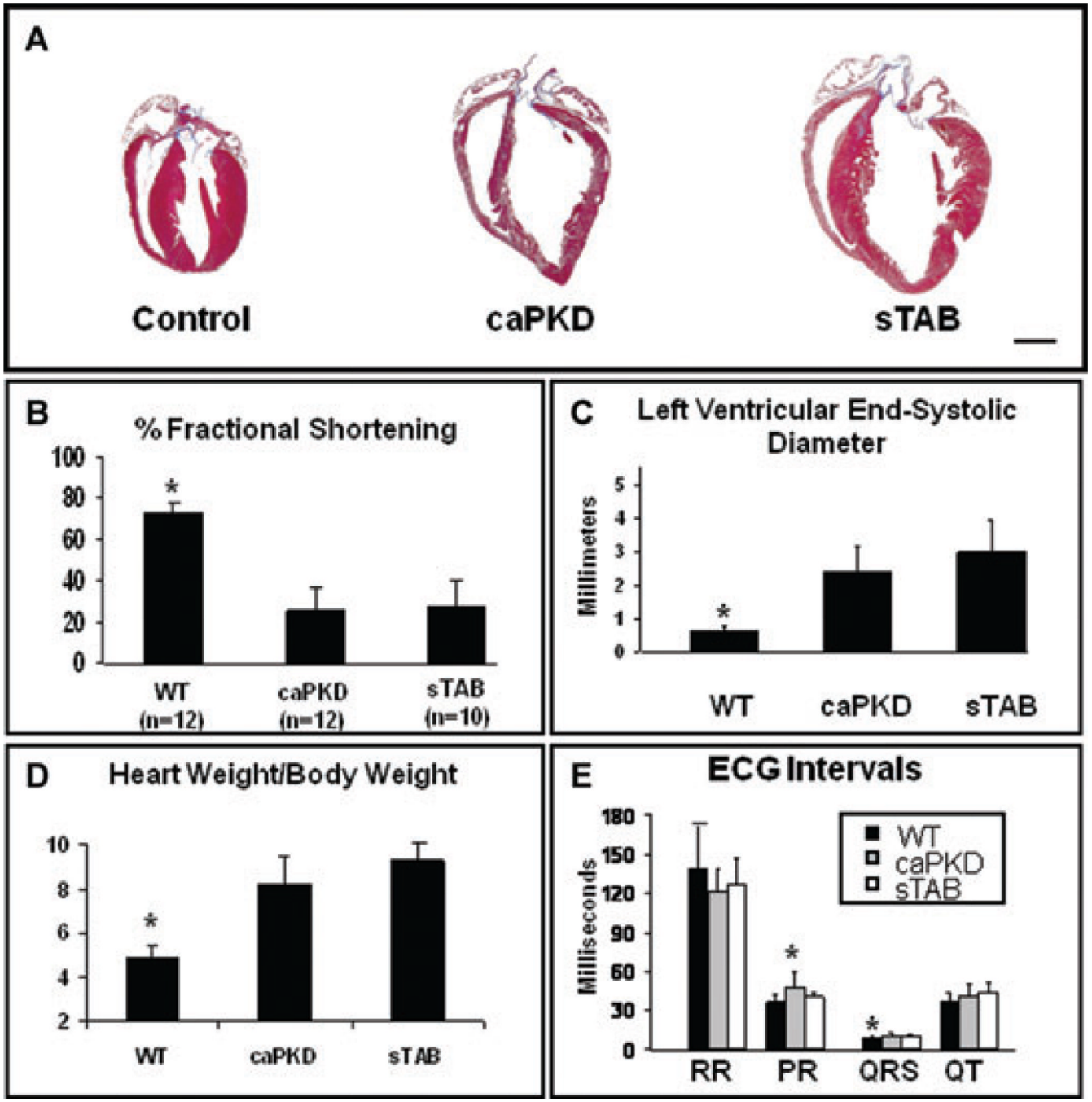

Figure 1.

(A) Representative histological heart sections from WT, caPKD, and sTAB-operated animals showed similar degrees of cardiac enlargement and dilation in sTAB-operated and caPKD transgenic animals. Echocardiographic assessment based on M-mode images showed significantly depressed left ventricular function in both the sTAB and caPKD mice (B) and comparable increases in the left ventricular systolic diameters (C). Assessment of heart mass revealed comparable increases in heart weight to body weight ratio in sTAB and caPKD mice (D). PR interval was slightly prolonged in caPKD mice as compared with WT and sTAB animals, and QRS interval was shorter in WT animals as compared with sTAB and caPKD animals. There were no significant differences between the groups in various

other electrocardiographic intervals, under resting sedated conditions (E). Vertical bars represent S.E.M. * denotes $P < 0.05$. Bar of measure equals 2 mm.

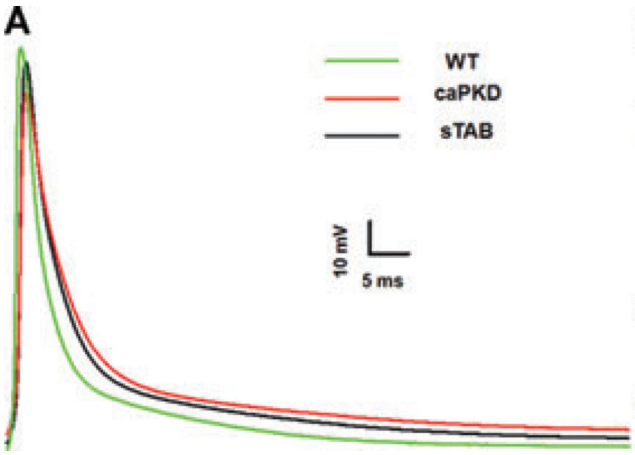

B

	WT (n=5, 9 cells)	caPKD(n=2, 5 cells)	sTAB(n=3, 6 cells)
RMP (mV)	-70±2	-70±2	-71 ± 2
Peak (mV)	43.8±2.5	42.6±3.5	43.6±1.5
APD30 (ms)	3.4±0.6	5.1±0.4*	5.0±0.2*
APD90 (ms)	15.2±3.2	25.7±4.5*	26.7±4.0*

Figure 2.

(A) Representative action potentials recorded from LV myocytes in WT, CaPKD, and sTAB mice. (B) Summary of the resting and active membrane properties of LV myocytes in WT, CaPKD, and sTAB mice. * denotes $P < 0.05$, compared with WT.

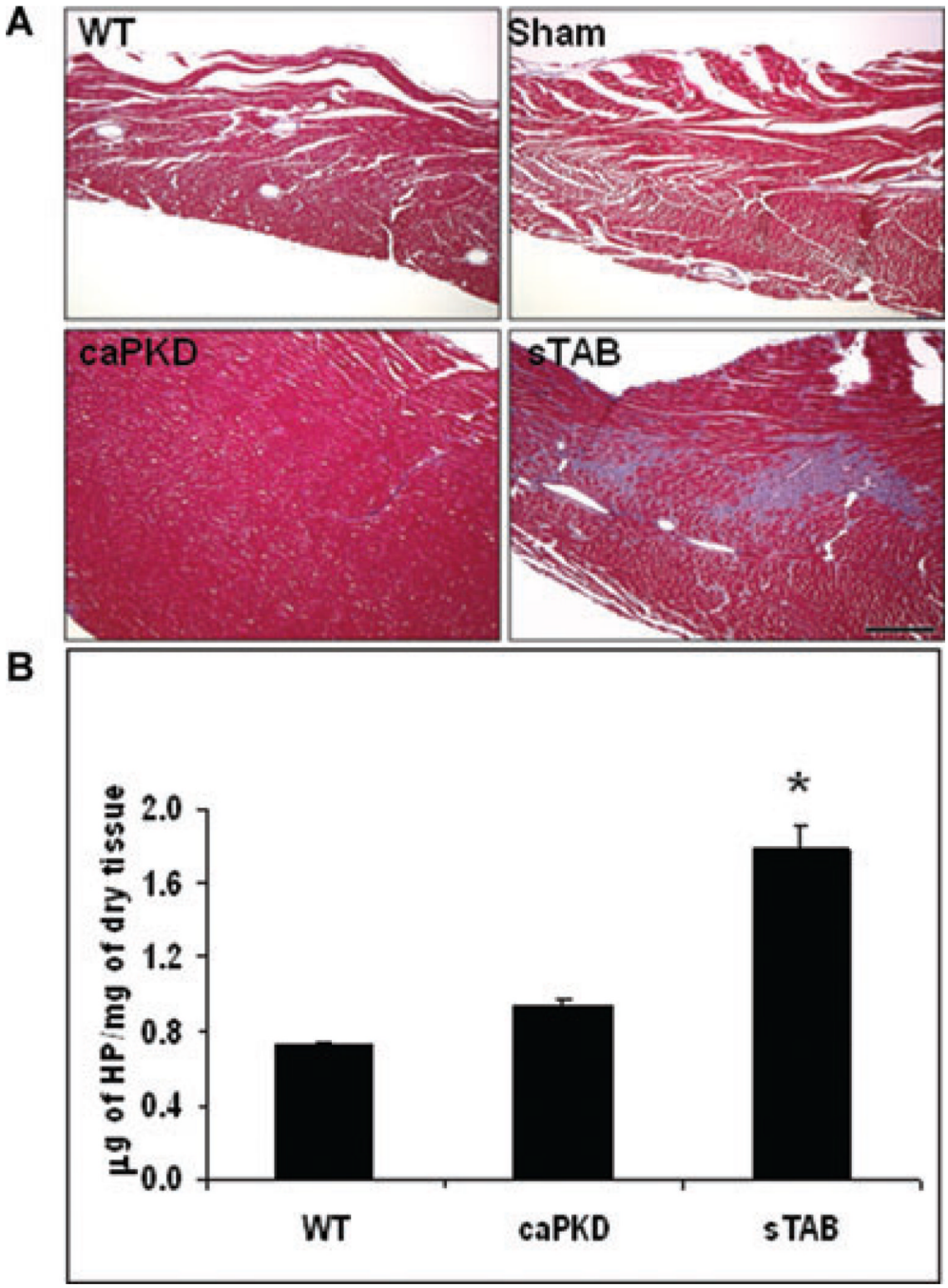

Figure 3.

(A) Representative Masson's trichrome-stained histological heart sections from WT, Sham-operated, sTAB-operated, and caPKD transgenic animals. Histologically, caPKD hearts had diminished fibrosis as compared with sTAB hearts, whereas Wild type and Sham-operated animals showed no evidence of collagen deposition in the heart. (B) Quantification of collagen, using hydroxyproline assay, showed decreased amounts of collagen in caPKD hearts as compared with sTAB animals. Vertical bars represent S.E.M. * denotes $P < 0.05$. Bar of measure equals 200 μm.

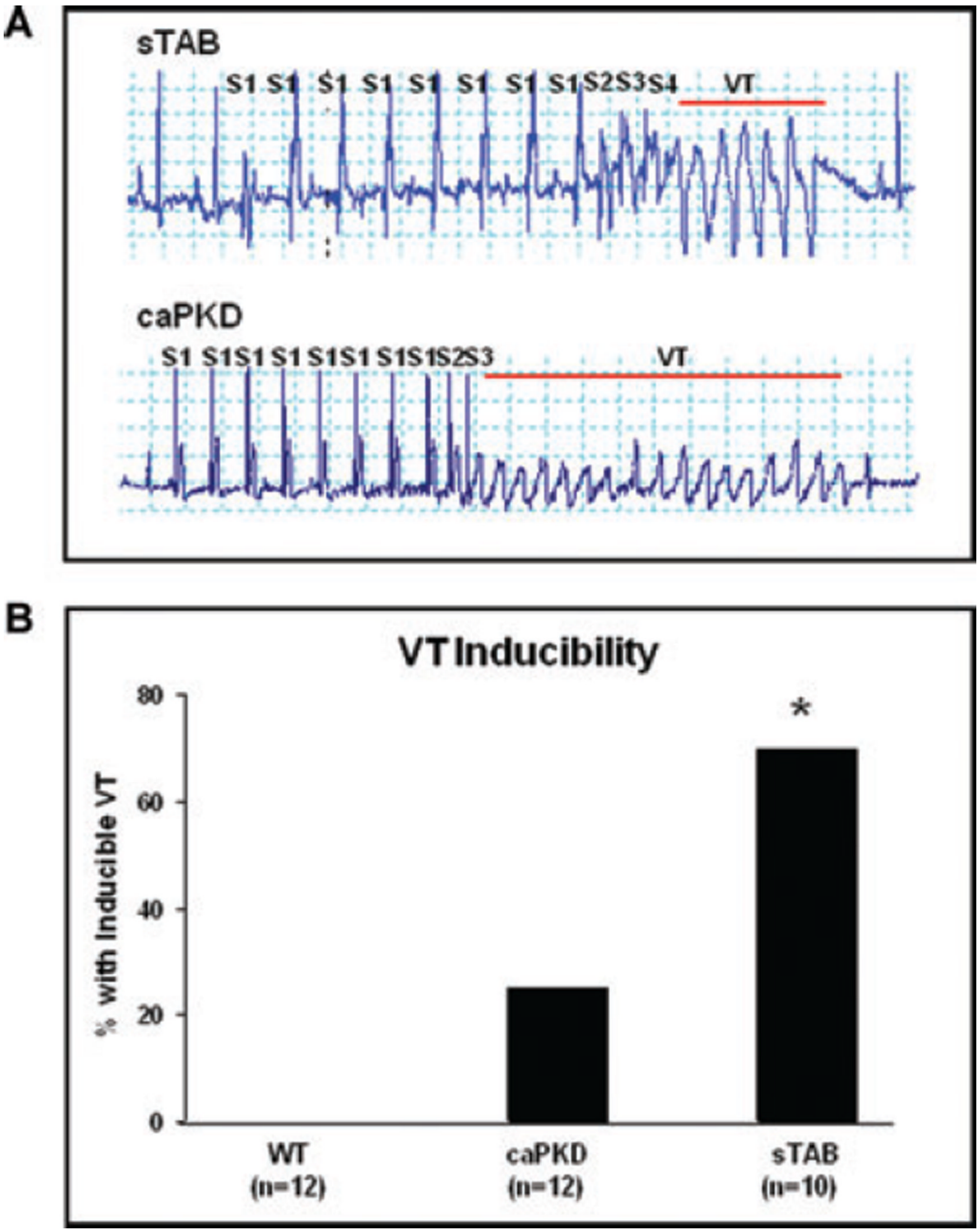

Figure 4.

(A) Shown is a representative image of induced ventricular tachycardia in sTAB and caPKD hearts. Electrophysiological evaluation, including comprehensive programmed electrical stimulation with and without isoproterenol, revealed significantly less amount of induced ventricular arrhythmias in caPKD mice as compared with sTAB animals (B). * denotes $P < 0.05$. Bar of measure equals 200 milliseconds.

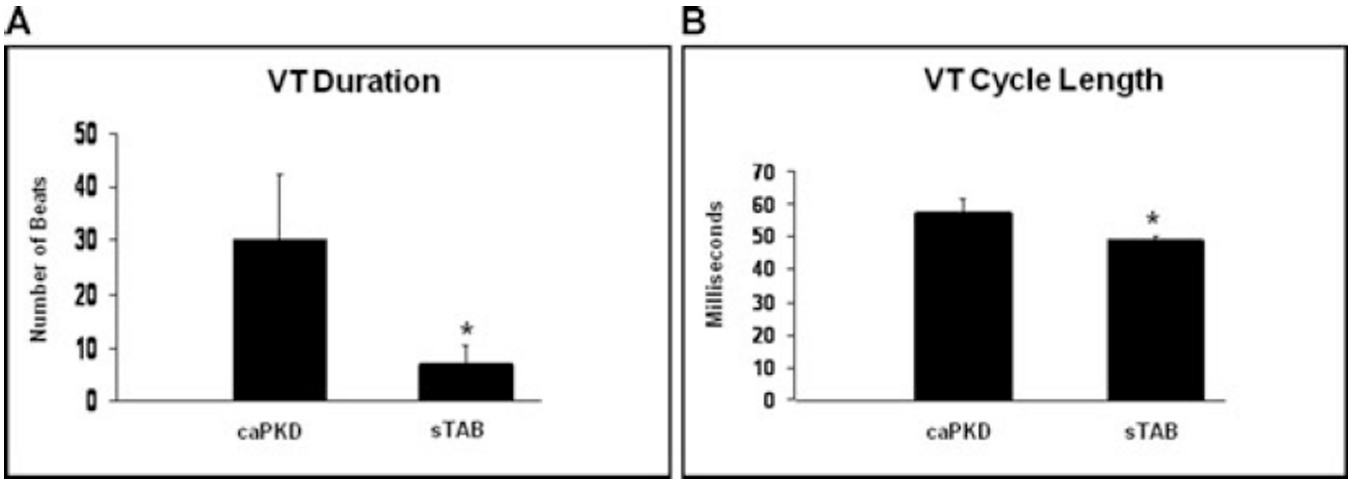

Figure 5.

(A) The duration of induced ventricular tachycardia was significantly longer in caPKD mice as compared with sTAB animals. (B) Cycle length analysis of induced arrhythmias revealed that ventricular tachycardia was slower in caPKD mice as compared with sTAB animals. Vertical bars represent SEM. * denotes $P < 0.05$.